

Scalable simultaneous multi-qubit readout with 99.99% single-shot fidelity

A. H. Burrell, D. J. Szwer, S. C. Webster and D. M. Lucas

Department of Physics, University of Oxford, Clarendon Laboratory, Parks Road, Oxford OX1 3PU, U.K.

(Dated: submitted 23 June 2009; this version 12 March 2010)

We describe single-shot readout of a trapped-ion multi-qubit register using space and time-resolved camera detection. For a single qubit we measure $0.9(3) \times 10^{-4}$ readout error in $400 \mu\text{s}$ exposure time, limited by the qubit's decay lifetime. For a four-qubit register (a “qunybble”) we measure an additional error of only $0.1(1) \times 10^{-4}$ per qubit, despite the presence of 4% optical cross-talk between neighbouring qubits. A study of the cross-talk indicates that the method would scale with negligible loss of fidelity to ~ 10000 qubits at a density $\lesssim 1$ qubit/ μm^2 , with a readout time $\sim 1 \mu\text{s}$ /qubit.

PACS numbers: 03.67.-a, 37.10.Ty, 42.50.Dv, 42.30.Va

Single-shot qubit readout is an essential requirement for quantum computing, in particular for implementing quantum error-correction [1] or measurement-based quantum computing [2]. Fault-tolerant quantum computing requires readout fidelities $\gtrsim 99.9\%$ if a large increase in the number of physical qubits per logical qubit is to be avoided [3]. Two major issues in scaling up from single-qubit to many-qubit systems are the need to perform operations on many qubits in parallel [1], and to overcome errors due to “cross-talk” between different qubits. In this paper we describe simultaneous readout on a multi-qubit register and show that the quantum state can be accurately inferred even in the presence of significant cross-talk. Since the latter is short-range, the method is scalable to much larger numbers of qubits.

For any physical implementation, readout error is usually limited by the time available to integrate a detector signal (to improve the signal-to-noise ratio) before the qubit decays. In recent work on a two-electron spin qubit in a double quantum dot, for example, the trade-off was between electronic measurement noise and the $34 \mu\text{s}$ qubit lifetime [4]. Cross-talk in a multi-qubit system could increase the measurement noise and/or decrease the qubit lifetime. In trapped-ion or neutral-atom approaches to quantum computing, qubit readout is usually achieved by driving a fluorescing cycling transition which involves one of the qubit states but not the other, and measuring whether or not the atom fluoresces [5]. Here the noise is predominantly photon-counting shot noise and the qubit lifetime is limited by spontaneous decay or off-resonant excitation, which can transfer the qubit from the “dark” state to the “bright” state or vice versa. Previous work reported measurement fidelities of 90%–98% for two- and three-qubit systems [6–8].

The highest fidelity quantum logic gate demonstrated to date [9] used a trapped-ion optical qubit stored in the $(4S_{1/2}, 3D_{5/2})$ levels of $^{40}\text{Ca}^+$, fig. 1a. For the same qubit, we have already described single-shot readout with 99.991(1)% fidelity for a single ion, using time-resolved detection of photons counted with a photomultiplier tube (PMT) [10]. Here, we extend this to simultaneous readout of multiple qubits using an electron-multiplying charge-coupled device (EM-CCD) camera, which allows both space- and time-resolved detection.

We first measure the readout error for a single qubit and find that, as with the PMT, at any given photon collection efficiency this is limited by the decay lifetime $\tau = 1168(7)$ ms of the metastable $D_{5/2}$ level [11]. Then we measure the readout error for a four-ion “qunybble” [12], where we eliminate the effect of the $D_{5/2}$ decay by post-selecting data, to find the residual error due to cross-talk between the imperfectly imaged ions.

The linear ion trap apparatus [11] and the methods for preparing and detecting the bright $S_{1/2}$ and dark $D_{5/2}$ qubit states are similar to those in [10], with the PMT replaced by the camera. Fluorescence at 397 nm from the ion(s) is collected by a compound objective of numerical aperture $\sin \alpha = 0.25$ and imaged onto the camera with net efficiency 1.0(1)%. The objective is not optimized for

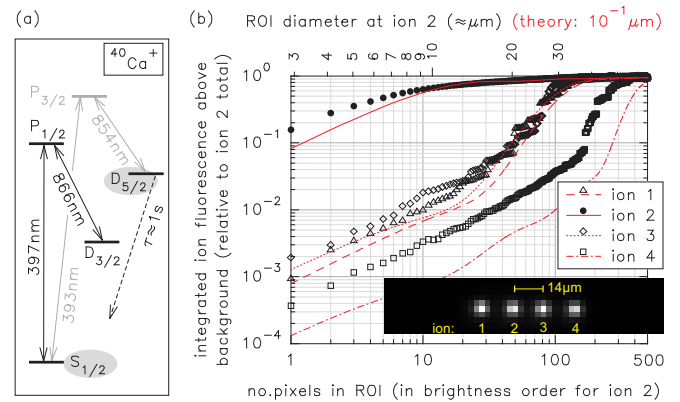


FIG. 1: (a) $^{40}\text{Ca}^+$ levels. (b) Image cross-talk affecting ion 2 in a string of four ions (inset: 50×10 pixel acquisition area, at scale $2.6 \mu\text{m}/\text{pixel}$). Filled circles show the integrated fluorescence from ion 2; the decreasing-brightness pixel order and data were obtained by averaging images in which only ion 2 was fluorescing. For the other three ions (hollow symbols) the same pixels were taken in the same order, but the data were taken from images in which only that ion was fluorescing. Up to ~ 100 pixels, the region-of-interest (ROI) is roughly circular, centred on ion 2, with a diameter in the object plane given by the upper abscissa. The lines show calculated performance for a diffraction-limited imaging system of the same numerical aperture, with ion spacings *ten times smaller* than in the image, on a $10\times$ magnified upper abscissa.

397 nm, resulting in performance well below the diffraction limit (fig. 1b). The nominal quantum efficiency (QE) of the camera at 397 nm is 48%, approximately twice that of the PMT. However, the stochastic gain process in the camera’s EM register leads to an excess noise factor of $\sqrt{2}$ above shot noise when operated at high gain, equivalent to an effective reduction in QE by a factor 2 for photon counting applications [13]. Background counts are dominated by the camera’s clock-induced charge (CIC) readout noise rather than by scattered light, but the finite qubit lifetime is still the principal limitation to readout fidelity. Cosmic rays cause fewer errors for the CCD than the PMT [10], due to its spatial discrimination.

We define the average readout error per qubit as $\epsilon = \frac{1}{2}(\epsilon_B + \epsilon_D)$, where ϵ_B is the fraction of experiments in which an ion prepared in the bright state was detected to be dark, and similarly for ϵ_D . In the single-qubit experiments described below, there is a small population preparation error for the dark state [10], resulting in a contribution to ϵ of $0.13(1) \times 10^{-4}$; values of ϵ given below are after subtraction of this quantity. In the four-qubit experiment the state preparation error is expected to be negligible because post-selection is used.

The readout fidelity for a single ion was measured by repeatedly preparing and measuring each qubit state, and comparing the measurement result with the known state preparation, for a total of 103744 trials. The method is similar to that described in [10], except that the time-resolved PMT detection bin is replaced by a single $400 \mu\text{s}$ camera exposure. Camera images were analysed both by simple pixel-count thresholding and by maximum likelihood techniques. We label the pixels $i = 1 \dots N$ in order of decreasing average brightness (determined from a long-exposure image, fig. 2a) and select a region-of-interest (ROI) by varying N .

For the threshold analysis method, we histogram the total pixel counts $\sum_{i=1}^N n_i$ where n_i is the photon count for pixel i , separately for the bright and dark state preparations, and choose the count threshold which optimizes discrimination between the histograms (fig. 2b, inset). The variation of ϵ with ROI size N is shown in fig. 2b; it decreases with N as the histogram overlap falls, reaches a minimum $\epsilon = 0.9(3) \times 10^{-4}$ (with $\epsilon_B = 0$) for $N = 28$, then eventually rises when the ROI is too large due to increasing background counts from pixels far from the ion which contain negligible information.

The simple threshold method does not take into account the known spatial distribution of the ion fluorescence over the ROI. In the “spatial” maximum likelihood analysis, we consider the likelihood $p_B = \prod_{i=1}^N B_i(n_i)$ that the set of pixel counts $\{n_i\}$ came from a bright ion, and compare this to the likelihood $p_D = \prod_{i=1}^N D_i(n_i)$ that $\{n_i\}$ arose from a dark ion. Here $B_i(n_i)$ is the probability of observing n_i counts on pixel i for a bright ion; similarly for D_i . Since the probability distribution B_i is different for each pixel, the information contained in the spatial distribution of the fluorescence is used. The distributions B_i and D_i can be obtained from indepen-

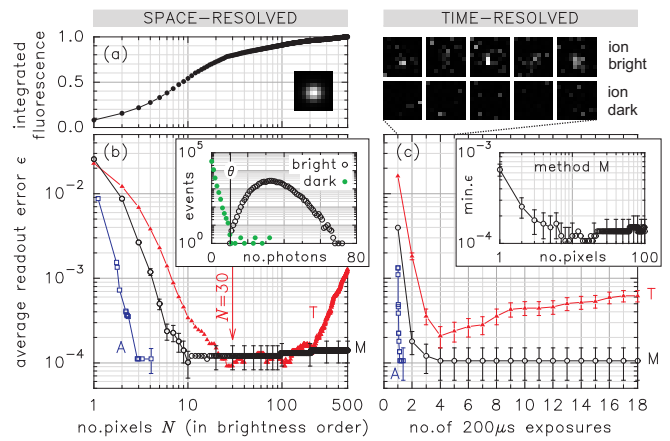


FIG. 2: Single-ion readout results for space- and time-resolved detection. Analysis methods: (T)hreshold, (M)aximum likelihood, (A)adaptive maximum likelihood. (a) Integrated fluorescence signal and long-exposure image. (b) Single $400 \mu\text{s}$ exposure: readout error ϵ versus ROI size N (inset: bright and dark photon count histograms for $N = 30$, with threshold θ). (c) Time-resolved detection using multiple $200 \mu\text{s}$ exposures with, above, example exposures 1–5 for bright and dark state preparation (inset: minimum ϵ versus N for method M).

dent control data, or by fitting the distributions from the experiment itself; either approach gave similar results. Maximum likelihood analysis results are also shown in fig. 2b; the minimum value of $\epsilon = 1.0(4) \times 10^{-4}$ is achieved with an ROI of only $N = 10$ pixels, demonstrating that the maximum likelihood technique is more efficient than the threshold method. However, it does not lead to a lower ϵ as this is limited by the $D_{5/2}$ decay.

An adaptive detection method (analogous to that described in [7, 10]) can reduce further the *average* number of pixels \bar{N} required to determine the qubit state. The *estimated* probability of measurement error can be inferred from p_B and p_D . For reliable readout, we only need use sufficient pixels for the absolute log-likelihood ratio $R = |\ln(p_B/p_D)|$ to be above some chosen confidence level. Taking the pixels in brightness order ensures most efficient use of the information. This method reaches the same ϵ in $\bar{N} = 2.9$ pixels, fig. 2b.

We also investigated time-resolved detection [14] for a single qubit. In this experiment, the single $400 \mu\text{s}$ camera exposure was replaced by a series of 18 exposures, each of duration $t_s = 200 \mu\text{s}$, to investigate whether time-resolved detection could give an improvement in readout fidelity by detecting any of the $D_{5/2}$ decays which limited the single-exposure fidelity. The method is similar to that used for PMT detection in [10], except that the CIC noise associated with reading each exposure from the CCD means that it is disadvantageous to make each exposure too short. The CCD itself was used to store all 18 exposures, allowing a rapid sequence of images with minimal dead time ($6 \mu\text{s}$) between each. Alternate bright and dark state preparations gave a total of 67892 trials (≈ 1.2 million exposures), which were analysed by simple

thresholding and by maximum likelihood analysis taking into account the effect of $D_{5/2}$ decay, with results shown in fig. 2c. For the “spatio-temporal” maximum likelihood analysis we compared the likelihoods $p_B = \prod_{j=1}^M p_{Bj}$ and

$$p_D = \left(1 - \frac{Mt_s}{\tau}\right) \prod_{j=1}^M p_{Dj} + \left(\frac{t_s}{\tau}\right) \sum_{j'=1}^M \prod_{j=1}^{j'-1} p_{Dj} \prod_{j=j'}^M p_{Bj}$$

which allows for the probability (t_s/τ) of spontaneous decay in exposure j' of M (see [10]). The probability p_{Bj} that exposure j came from a bright ion is given by $p_{Bj} = \prod_{i=1}^N B_{ji}(n_{ji})$ where $B_{ji}(n_{ji})$ gives the probability of measuring n_{ji} counts on pixel i of exposure j for a bright ion; similarly for p_{Dj} . The minimum error is $\epsilon = 1.1(4) \times 10^{-4}$, for $M \geq 4$ exposures, no lower than the single-exposure experiment. A (temporally) adaptive analysis is also shown in fig. 2c, and reaches the same ϵ in an average of $\bar{M} = 1.1$ exposures ($230 \mu\text{s}$); however the overhead in CCD read time for multiple exposures means the adaptive technique offers little practical speed-up.

We now describe an experiment to measure the readout error ϵ_X for the four-ion qunybble, independently of the $D_{5/2}$ decay error. The cross-talk due to imperfect imaging in our system is illustrated in fig. 1b, where the data were taken from the experiment to be described below. For an ROI centred on ion 2 with diameter equal to the mean ion spacing of $14 \mu\text{m}$, the nearest neighbour ions each contribute signals $\approx 4.0\%$ of the signal from ion 2 itself, while the next-nearest neighbour contributes 0.9% . Cross-talk at this level could clearly impact the readout error at the 10^{-4} level achieved for a single ion.

We are not able to prepare all 16 possible qunybble states $\{0000, \dots, 1111\}$ deterministically with an error $\sim 10^{-5}$ as in the single-qubit experiments above. Instead, in each trial we prepare a random qunybble state, and sandwich the readout test measurement between “pre” and “post” measurements. We then select for analysis only those trials in which the “pre” and “post” measurements agree: these measurements give the state that was prepared, to which the “test” measurement is compared. A dark \rightarrow bright decay from the $D_{5/2}$ level during the trial will cause the “pre” and “post” measurements to disagree for the ion which decayed. By increasing the exposure time of the “pre” and “post” measurements only, we increase the accuracy of this state post-selection procedure at the expense of rejecting more trials.

A single trial consists of 6 identical camera exposures each of $400 \mu\text{s}$ duration (fig. 3a), with the CCD being read out between each. An initial “check” exposure is taken with all ions fluorescing. Then a short ($12 \mu\text{s}$) pulse of 393nm light shelves the ions in $D_{5/2}$ with a probability 0.46 per ion, to prepare a random qunybble state (with each state approximately equally probable, inset fig. 3b). The next two exposures are added to give the “pre” measurement, the fourth exposure constitutes the actual readout “test” measurement, and the last two exposures are added for the “post” measurement. Finally an 854nm laser pulse returns all ions to the bright state.

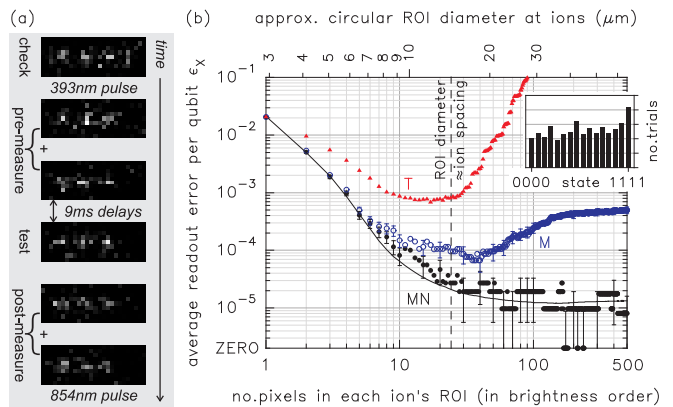


FIG. 3: Four-ion readout experiment. (a) Experimental sequence, showing a typical trial; maximum likelihood analysis applied to the $400 \mu\text{s}$ “test” exposure gives the qunybble state as $\{1110\}$ with estimated probability of error $\approx \sum_{k=1}^4 e^{-R_k} = 1.4 \times 10^{-11}$. (b) Readout error per qubit averaged over trials of all 16 qunybble states $\{0000, \dots, 1111\}$, whose distribution is shown in the inset. The error due to $D_{5/2}$ decay is excluded as described in the text. Analysis methods: (T)hreshold; (M)aximum likelihood ignoring neighbours; (MN) iterative maximum likelihood method taking into account nearest neighbours, with (solid line) a Monte-Carlo simulation of 10^9 trials. Adjacent ROIs overlap when their diameters exceed the $14 \mu\text{m}$ mean ion spacing.

This sequence was repeated 30100 times, giving 120400 qubit trials. We first identify those trials where the “pre” and “post” measurements disagree, and discard them, using thresholding of pixel counts summed over rectangular ROIs. Two thresholds were used to improve our confidence in the retained trials: we demand either that the “pre” and “post” measurements are *both* above the upper threshold, or that *both* are below the lower threshold. The separation between the upper and lower thresholds was such that 95% of trials were retained [16].

Having thus selected a set of trials with known qubit states, we proceed to analyse the “test” exposures. We first apply a simple threshold analysis, treating each ion independently. The pixel counts n_{ki} for each ion k are summed over independent brightness-order ROIs, and an independent threshold is chosen for each ion. The minimum readout error (per qubit) is $\epsilon_X = 6.8(8) \times 10^{-4}$ (fig. 3b) and ϵ_X rises rapidly above $N \approx 25$ pixels, where the ROI diameters exceed the mean ion spacing.

The spatial maximum likelihood analysis should be more immune to the effects of image cross-talk since it requires fewer pixels and gives less weight to pixels further from the ion of interest. For each ion k we compare the likelihoods $p_B = \prod_{i=1}^N B_{ki}(n_{ki})$ and $p_D = \prod_{i=1}^N D_{ki}(n_{ki})$ that the set of counts $\{n_{ki}\}$ came from a bright or dark ion, where $B_{ki}(n_{ki})$ is the probability of observing n_{ki} counts on ion k ’s i th brightest pixel when that ion is bright, and similarly for $D_{ki}(n_{ki})$. The probability distributions B_{ki} and D_{ki} are obtained from the “pre” and “post” exposures only and are thus independent of the

“test” exposures. Results are shown in fig. 3b and reach an error $\epsilon_X = 0.7(3) \times 10^{-4}$ per qubit, an order of magnitude below simple thresholding. As expected, the error is less sensitive to the ROI overlapping neighbouring ions.

Nevertheless, we can improve the analysis by taking into account the effect of neighbouring ions explicitly. There is a significant effect on the dark distribution D_k depending on whether the neighbour k' is bright or dark; indeed for a pixel far from ion k but close to ion k' the shape of the distribution will be dominated by the state of k' even though the pixel may still contain useful information on the state of k . To extract this information, we now allow independent probability distributions $B_{\nu ki}(n_{ki})$ and $D_{\nu ki}(n_{ki})$ for each neighbour state $\{\nu\} = \{00, 01, 10, 11\}$. These distributions are again found using the “pre” and “post” exposures only, where we know the state of both ion k and its neighbours $\{\nu\}$. However, when we use these distributions to analyse a particular “test” exposure we do *not* assume any knowledge of the neighbour states: instead we proceed iteratively, making an initial guess for the qunybble state of $\{0000\}$, measuring the state of each qubit k with $\{\nu\} = \{00\}$, recalculating using the neighbour states from the first iteration to give a second measurement, and so on until the inferred qunybble state is stable. Results from this iterative maximum likelihood analysis are also plotted in fig. 3b: for ROI size $N \geq 60$ pixels the readout error per qubit reaches an average level of $\epsilon_X = 0.1(1) \times 10^{-4}$ and is even zero (in 114606 trials) for certain N . There is now no penalty for allowing the ROI to overlap neighbouring ions. The agreement with the simulation in fig. 3b indicates that systematic effects (e.g., correlated errors common to “pre”, “post” and “test” exposures) are below the statistical uncertainty.

Finally we can search for effects due to non-nearest neighbours by generalizing the preceding analysis to neighbour states $\{\nu\} = \{000, \dots, 111\}$, which allows for all permutations of the three neighbour ions to any ion k . We find no reduction in ϵ_X or N and conclude that any effect is at or below the $\sim 10^{-5}$ level.

The single-ion experiment achieved a readout fidelity of 99.991(3)% with a single 400 μs camera exposure, limited by the photon collection efficiency and the lifetime of the $D_{5/2}$ qubit state. The four-ion qunybble experiment demonstrated that, when the effects of the $D_{5/2}$ decay are excluded, discrimination accuracy of 99.999(1)%

can be achieved with the same exposure time, even in the presence of significant image cross-talk from neighbouring ions. Together these two experiments imply that 99.99% net fidelity can be attained with the camera for simultaneous multiple qubit readout. Since it was found sufficient to include only the effects of nearest neighbors, this result should extend to one-dimensional qubit registers of arbitrary length, given comparable imaging quality over the entire ion string. As the error due to neighbour effects is small ($\epsilon_X \ll \epsilon$), the fidelity should be similar even for a 2D array of ions (or neutral atoms in a long-wavelength optical lattice [15], given the same fluorescence and dark \leftrightarrow bright rates). This 512×512 pixel camera could be used to measure a 2D array of at least 10000 qubits simultaneously; the exposure time would then be negligible compared with the CCD readout time ($\sim 1 \mu\text{s}$ per qubit at the fastest available readout speed of $0.1 \mu\text{s}/\text{pixel}$). A CCD which allowed parallel pixel readout would offer a significant speed-up. Image processing time is $< 0.1 \mu\text{s}/\text{pixel}$, so the main classical computing resource cost is storage ($\sim 1 \text{ kB}/\text{pixel}$) for the B_i and D_i distributions.

The cross-talk in our system was limited by imperfections in the imaging system. To estimate what is theoretically possible, we plot on fig. 1b the calculated image cross-talk for a diffraction-limited imaging system at $\lambda = 397 \text{ nm}$ with the same numerical aperture $\sin \alpha = 0.25$, but with ion spacings reduced by a factor of 10. The cross-talk from neighbouring ions was calculated by integrating the Airy pattern over off-axis circular ROIs, and is qualitatively similar to our measured cross-talk. In this calculation the spacing between the ions, $1.4 \mu\text{m}$, is less than the diameter of their Airy discs $\approx 1.22\lambda/\tan \alpha = 1.9 \mu\text{m}$. The implication is that readout fidelity at the 99.99% level is attainable for ions or atoms spaced close to the diffraction limit, with an imaging system possessing the same collection efficiency.

We thank Andor Technology for the loan of the camera (model DU-897), and other members of the Oxford ion trap group (particularly D. N. Stacey and A. M. Steane) for helpful discussions. This work was funded by EPSRC (QIP IRC), IARPA (ref. 47968-PH-QC), the European Commission (SCALA, MicroTrap) and the Royal Society.

Related experiments have recently been performed by F. Zähringer and co-workers at Innsbruck University.

-
- [1] A. M. Steane, *Quant. Inf. Comp.* **7**, 171 (2007).
 - [2] M. A. Nielsen, *Rep. Math. Phys.* **57**, 147 (2006).
 - [3] E. Knill, *Nature* **434**, 39 (2005).
 - [4] C. Barthel *et al.*, *Phys. Rev. Lett.* **103**, 160503 (2009).
 - [5] D. J. Wineland *et al.*, *Opt. Lett.* **5**, 245 (1980).
 - [6] M. Steffen *et al.*, *Science* **313**, 1423 (2006).
 - [7] D. B. Hume *et al.*, *Phys. Rev. Lett.* **99**, 120502 (2007).
 - [8] M. Acton *et al.*, *Quant. Inf. Comp.* **6**, 465 (2006).
 - [9] J. Benhelm *et al.*, *Nature Physics* **4**, 463 (2008).
 - [10] A. H. Myerson *et al.*, *Phys. Rev. Lett.* **100**, 200502 (2008).
 - [11] P. Barton *et al.*, *Phys. Rev.* **A62**, 032503 (2000).
 - [12] A nybble is half a byte, hence a qunybble is four qubits; see J.-Å. Larsson, *Phys. Rev. A* **69**, 042317 (2004).
 - [13] C. D. Mackay *et al.*, *Proc. SPIE* **4306**, 289 (2001).
 - [14] C. Langer, Ph.D. thesis, University of Colorado (2006).
 - [15] K. D. Nelson *et al.*, *Nature Physics* **3**, 556 (2007).
 - [16] A single threshold keeps 99% of trials, and gives $\epsilon_X = 0.3(2) \times 10^{-4}$.